External fields on the nightside of Mars at Mars Global Surveyor mapping altitudes

B. B. Ferguson,[1] J. C. Cain,[1] D. H. Crider,[2] D. A. Brain,[3] and E. M. Harnett[4]

Received 11 November 2004; revised 8 June 2005; accepted 23 June 2005; published 26 August 2005.

[1] More than four years of data taken from Mars Global Surveyor during its Mapping Phase Orbits (360–420 km altitude) over low field regions were examined. The nightside magnetic field data were binned according to a proxy solar wind pressure calculated from the dayside measurements. When the crustal field contribution calculated from the internal field model (FSU90) is removed, the distribution of residuals is bi-valued in the sunward component. Pass-by-pass inspections of the data sometimes show a sudden reversal of field, which occur on successive passes. Analysis indicates that for these orbits MGS traverses a current sheet that separates the two lobes of Mars' magnetotail. These results indicate that on the nightside the major contributor to the external field is the draping of the Interplanetary Magnetic Field about the planet and that care must be taken when utilizing such data for modeling Mars' internal field. **Citation:** Ferguson, B. B., J. C. Cain, D. H. Crider, D. A. Brain, and E. M. Harnett (2005), External fields on the nightside of Mars at Mars Global Surveyor mapping altitudes, *Geophys. Res. Lett.*, *32*, L16105, doi:10.1029/2004GL021964.

1. Introduction

[2] Much has been learned of Mars' magnetic field since the arrival of the Mars Global Surveyor (MGS), both of its strong crustal magnetization [*Acuña et al.*, 1999] as well as its interactions with the solar wind and the IMF. *Cloutier et al.* [1999] outlined a number of similarities between Mars and Venus in regards to their solar wind interactions, such as the existence of a Magnetic Pile-up Boundary (MPB), wave activity between the bow shock and the MPB, flux-rope formations, and the disappearance of the nightside ionosphere, while *Bertucci et al.* [2003] have shown magnetic field draping enhancement at the MPB. *Lundin and Barabash* [2004] have compared and contrasted the induced magnetotails of Mars and Venus caused by such draping, and *Nagy et al.* [2004] have summarized what is known of Mars' magnetotail, all relying mainly on data collected by Phobos-2. We add to such analyses here using data collected from MGS to investigate the effect of solar wind pressure on the morphology of Mars' induced magnetotail.

[3] Crustal field modeling relies on the isolation of fields originating in the interior of the planet from external contributions. On the dayside there are known increases of the absolute field due to pressure from the solar wind impinging on the planet's upper atmosphere [*Crider et al.*, 2004]. Most attempts to model the low-altitude details of the crustal field structures are forced to use dayside data because nearly all low altitude measurements (<200 km) were taken in daytime. Various authors [*Arkani-Hamed*, 2004; *Cain et al.*, 2003; *Hood et al.*, 2005; *Langlais et al.*, 2004] have modeled the internal magnetic field assuming that nightside data are the least disturbed by external sources. By "external" we mean contributions from the draped IMF and from currents flowing in the Martian ionosphere either by induction from solar wind interactions, or from ionospheric winds interacting with the crustal field. The last would be only possible over the regions where the crustal magnetic field is strong enough to interact with charged particle motion. In this study we avoid such regions.

[4] The purpose of this paper is to examine the morphology of magnetic fields in the near-tail region of Mars and extract the contributions from crustal sources and external fields. The data used in this study were taken from MGS Mapping Phase Orbit (MPO) magnetic field and electron reflection (MAG/ER) data. Based on the statistics of the residuals from an $n = 90$ internal field model, it is shown that over regions of low crustal fields the structure of the Martian magnetotail is controlled mainly by the draped IMF, with a bifurcation of the residuals along the Mars-Sun direction. In addition, evidence is provided for a magnetotail current sheet that extends as far inward as the MGS mapping altitudes. A study of a series of orbit-by-orbit passes sometimes shows a sudden reversal of the magnetic field which appears on successive orbits near the same latitude, consistent with a current sheet crossing.

2. MGS Data Analysis and Discussion

[5] Our analysis used all available magnetic field data (3 second averages) from day 67 of 1999 to day 6 of 2004. These data are calibrated to within ±1 nT when MGS is sunlit and ±0.5 nT in darkness [*Acuña et al.*, 2001]. During this time period, MGS was in a 2am–2pm mapping orbit near 400 km. Dayside data were used to determine a solar wind proxy pressure for each orbit. Analysis was then done on data that were chosen on the nightside of Mars away from the strong crustal field sources. In particular, the selection criterion: $|B|$ of the potential internal field, which is predicted by the 90-term spherical potential internal field model FSU90 [*Cain et al.*, 2003], is less than 10 nT has been applied. Only low field regions are considered here

[1]Geophysical Fluid Dynamics Institute and School of Computational Science, Florida State University, Tallahassee, Florida, USA.
[2]Physics Department, Catholic University of America, Washington, D. C., USA.
[3]Space Sciences Lab, University of California, Berkeley, California, USA.
[4]Department of Earth and Space Sciences, University of Washington, Seattle, Washington, USA.

0094-8276/05/2004GL021964$05.00

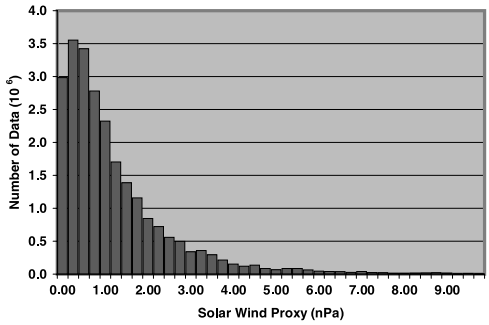

Figure 1. Distribution of magnetic field vectors binned according to proxy solar wind pressure in 0.25 nPa increments. See color version of this figure in the HTML.

because interactions of the crustal sources with the nightside plasma environment complicates the analysis of any external contributions to the field in the tail. MHD simulations by *Harnett and Winglee* [2005] show that the orientation of the strong magnetic anomalies influences the tail morphology.

[6] Using the method developed by *Crider et al.* [2003], upstream solar wind pressure was estimated for each orbit in the data set. The method assumes that the solar wind dynamic pressure p_{sw} is balanced by the magnetic field pressure in the magnetic pile-up region. The equation for the estimated solar wind pressure, p_{MGS} is given by:

$$p_{MGS} = \frac{B_{MPR}^2}{2\mu_0 k \cos^2\theta}, \quad (1)$$

where θ is angle between the ram direction and the obstacle surface normal, and k is a proportionality factor of 0.88. For the obstacle surface, the average MPB was used [*Vignes et al.*, 2000]. B_{MPR} is an estimate of the total external magnetic field measured on the dayside of Mars in the magnetic pile-up region. To obtain B_{MPR} we use the total magnetic field measurement on the dayside in regions away from strong crustal sources, including only data for which the average $|B|$ is less than or equal to 10 nT using a map developed by *Connerney et al.* [2001]. The solar wind pressure is calculated for each point and then averaged for each pass. Applying this method to the mapping data yields a range of proxy solar wind values from 0 to 10 nPa, and binning the data in 0.25 nPa increments leads to the distribution shown in Figure 1.

[7] The low-field, nightside data were then binned according to this proxy solar wind pressure, and the residuals were calculated in Sun state (SS) coordinates (B_{xSS}, B_{ySS}, B_{zSS}) using FSU90. In this coordinate system the x-axis is aligned in the sunward direction along the Mars-Sun line, the y-axis is aligned antiparallel to the orbital velocity of Mars, and the z-axis completes the right-handed set. This selection and binning yielded approximately 2.5×10^7 total vectors in SS coordinates.

[8] The data combined from all the bins were then reduced to 10^7 observations using the same equal-area technique as in the FSU90 derivation. As shown in Figure 2, histograms of these residuals for each of the Sun state coordinates show that while B_{ySS} and B_{zSS} are normal Gaussians with a width of about 5 nT, there is a strong bi-modal distribution in the sunward/tailward B_{xSS} component. In addition, the bins were combined into seven groups of increasing solar wind pressure such that each group contained approximately 3×10^6 data points. Figure 3 shows that the separation in the two peaks in the B_{xSS} distribution increases with increasing pressure, with the separation exceeding 30 nT for the highest upstream pressures. These general trends are also present in the data before subtracting the FSU90 fields. High pressures increase the external field magnitude which causes $|B_{xSS}|$ to be larger at higher pressures than at lower pressures, hence increasing the separation between the peaks.

[9] Note that the distributions are asymmetric, with more positive then negative residuals. On the nightside, positive B_xSS corresponds to a downward field. *Krymskii et al.* [2002] also noted an asymmetry in MGS data, with an excess of $-B_r$ (or $+B_xSS$) in the mapping nightside averages. It is as yet unclear whether this asymmetry is the effect of seasonal selection mentioned by *Krymskii et al.* [2002], an asymmetry in induced magnetosphere as noted by D. A. Brain and D. L. Mitchell (The magnetic field draping direction at Mars from April 1999 through August 2004, submitted to *Icarus*, 2005), or the effect of the strong crustal sources on the induced magnetotail.

[10] This asymmetry would undoubtedly lead to inaccuracies in those internal field models which rely on binning and averaging the MPO data [*Langlais et al.*, 2004; *Hood et al.*, 2004], as well as those models which use large sampling of the data (e.g., *Arkani-Hamed* [2002] and FSU90 itself) to minimize external effects. *Hood et al.* [2005] attempted to remove fluctuations by visually inspecting data on a pass-by-pass basis and therefore most likely reduced the amount of external

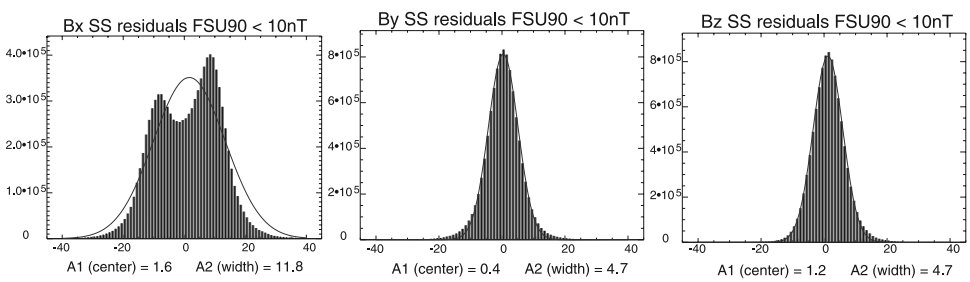

Figure 2. Histograms of the nightside Sun state magnetic field residuals over regions away from crustal anomalies for the entire data set reduced to 10^7 equal area points and least squares curve fit to distribution (solid line). Center and width of curve and horizontal scale in nT. See color version of this figure in the HTML.

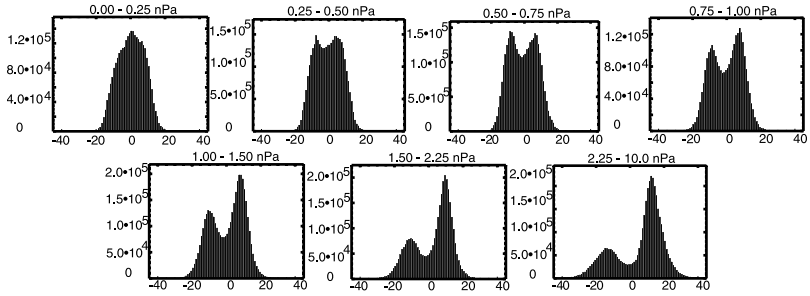

Figure 3. Histograms of the nightside Bx SS residuals binned according to the proxy solar wind pressure. The seven groups were selected to allow for approximately 3×10^6 equal area points per group. See color version of this figure in the HTML.

contribution, but it is unknown to what extent compared with other models. The altitude normalized maps of *Connerney et al.* [2001] also include this external contamination as they were generated by binning the data and selecting the median values in each bin. In any event, this analysis demonstrates the need for a new selection criterion for the MPO data when generating future internal field models. It is obvious that those orbits for which there is low upstream solar wind pressure and hence smaller external nightside contributions are most desirable. It may be that with such a selection discrepancies between various models (e.g., the power spectrum correlations discussed by *Arkani-Hamed* [2004]) would be minimized.

[11] In addition to statistical analysis, orbits were examined pass-by-pass for the period of days 230–250 of 2003. Certain orbits during this period showed sudden and drastic changes in the direction of the external field on the tailside of Mars. The sudden reversals were seen to occur on 26 of the 250 orbits in this time period. Of these 26, 5 reversals appear at similar latitudes on successive passes. Figure 4 shows an example of one such pass, orbit 8 day 234. The majority of the nightside reversal for this pass occurs in the B_{xSS} direction, and there is a sharp drop in $|B|$ at the polarity change.

[12] To more fully understand the nature of this sudden reversal, the residual vectors are rotated around x_{SS} to create a new coordinate system (x'_{SS}, y'_{SS}, z'_{SS}) in which the position MGS during the nightside reversal appears in the $x'_{SS} - z'_{SS}$ plane. In a draped field geometry, the $y'_{SS} = 0$ plane separates sunward from tailward directed magnetic field on both the dayside and the nightside. On the nightside, a current sheet is expected in the $y'_{SS} = 0$ plane, between the induced tail lobes. On the dayside, the magnetic field is primarily perpendicular to the $y'_{SS} = 0$ plane. However, the B'_{xSS} component slowly changes as a function of y'_{SS}, and is expected to pass through 0 at the $y'_{SS} = 0$ plane. As shown in Figure 4, when plotted in this coordinate system, a dayside reversal is also evident and located quite close to the $y'_{SS} = 0$, indicated by the vertical lines in the second column of Figure 4. This correlation in the positions of the dayside and nightside reversals indicates that the polarity shifts are due to IMF draping. In addition, electron flux data are plotted and show that indeed there is a small increase of flux in the

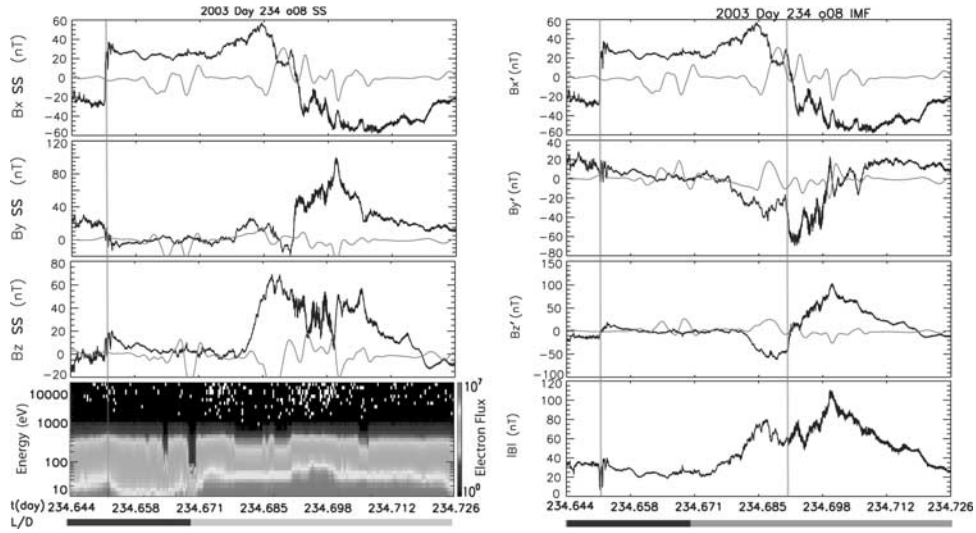

Figure 4. Residual data for day 234 of 2003 (orbit 8) plotted in SS and SS′ coordinates showing sudden reversal of field on the nightside. Vertical lines indicate the position of the nightside reversal in both coordinates as well as the corresponding dayside reversal in SS′ coordinates. The smooth curves are the predictions of FSU90. Electron flux data are shown in the bottom panel of the first column. Units of flux are $cm^{-2}s^{-1}ster^{-1}eV^{-1}$. The L/D panel indicates light/dark conditions. See color version of this figure in the HTML.

low energy channels at the time of the reversal. This signature is nearly identical for the following pass, orbit 9 (not shown). Based on this evidence it appears that the spacecraft passes through a current sheet separating the two lobes of an induced magnetotail. When plotted in planetocentric coordinates, the system normally utilized in field modeling, both the dayside and nightside reversals are evenly distributed across all components.

3. Conclusions

[13] It is apparent from the above observations that there are significant external contributions to the magnetic field at MPO altitudes even on the nightside of Mars. This has consequences for both the further modeling of the crustal sources and the understanding of Mars' magnetotail morphology. The double peaks in the B_{xSS} histograms show that the morphology of the tail is controlled by the draped IMF and solar wind pressure. The magnetic field flux in the sunward lobe of the Martian magnetotail is found to be significantly larger than in the anti-sunward lobe when the SW dynamic pressure is high. Based on the infrequency of the sudden field reversals it would appear that most of the time the spacecraft traverses through either a sunward or anti-sunward lobe, and only occasionally is the IMF aligned in such a way as to allow the spacecraft to pass through the current sheet that separates them.

[14] **Acknowledgment.** This work is supported under NASA grants NAG5-8284 and NAG5-12235.

References

Acuña, M. H., et al. (1999), Global distribution of crustal magnetization discovered by the Mars Global Surveyor MAG/ER experiment, *Science*, *284*, 790–793.

Acuña, M. H., et al. (2001), The magnetic field of Mars: Summary of results form the aerobraking and mapping orbits, *J. Geophys. Res.*, *284*, 403–423.

Arkani-Hamed, J. (2002), An improved 50-degree spherical harmonic model of the magnetic field of Mars derived from both high-altitude and low-altitude data, *J. Geophys. Res.*, *107*(E10), 5083, doi:10.1029/2001JE001835.

Arkani-Hamed, J. (2004), A coherent magnetic model of the Martian crust, *Eos Trans. AGU*, *85*(17), Jt. Assem. Suppl., Abstract P31A–03.

Bertucci, C., et al. (2003), Magnetic field draping enhancement at the Martian magnetic pileup boundary from Mars Global Surveyor observations, *Geophys. Res. Lett.*, *30*(2), 1099, doi:10.1029/2002GL015713.

Cain, J. C., B. Ferguson, and D. Mozzoni (2003), An n = 90 internal potential function of the Martian crustal magnetic field, *J. Geophys. Res.*, *108*(E2), 5008, doi:10.1029/2000JE001487.

Cloutier, P. A., et al. (1999), Venus-like interaction of the solar wind with Mars, *Geophys. Res. Lett.*, *26*, 2685–2688.

Connerney, J. E. P., M. H. Acuña, P. J. Wasilewski, G. Kletetschka, N. F. Ness, H. Rème, P. Lin, and D. L. Mitchell (2001), The global magnetic field of Mars and implications for crustal evlution, *Geophys. Res. Lett.*, *28*, 4015–4018.

Crider, D. H., D. Vignes, A. M. Krymskii, T. K. Breus, N. F. Ness, D. L. Mitchell, J. A. Slavin, and M. H. Acuña (2003), A proxy for determining solar wind dynamic pressure at Mars using Mars Global Surveyor data, *J. Geophys. Res.*, *108*(A12), 1461, doi:10.1029/2003JA009875.

Crider, D. H., D. A. Brain, M. H. Acuña, D. Vignes, C. Mazelle, and C. Bertucci (2004), Mars Global Surveyor observations of solar wind magnetic field draping around Mars, *Space Sci. Rev.*, *111*, 203–221.

Harnett, E. M., and R. M. Winglee (2005), Three-dimensional fluid simulations of plasma asymmetries in the Martian magnetotail caused by the magnetic anomalies, *J. Geophys. Res.*, *110*, A07226, doi:10.1029/2003JA010315.

Hood, L. L., C. N. Young, N. C. Richmond, and K. P. Harrison (2005), Modeling of major Martian magnetic anomalies: Further evidence during the Nochian, *Icarus*, in press.

Krymskii, A. M., T. K. Breus, M. H. Acuna, J. E. P. Connerney, D. H. Crider, D. L. Mitchell, and S. J. Bauer (2002), Structure of the magnetic field fluxes connected with crustal magnetization and top-side ionosphere at Mars, *J. Geophys. Res.*, *107*(A9), 1245, doi:10.1029/2001JA000239.

Langlais, B., M. E. Purucker, and M. Mandea (2004), Crustal magnetic field of Mars, *J. Geophys. Res.*, *109*, E02008, doi:10.1029/2003JE002048.

Lundin, R., and S. Barabash (2004), The wakes and magnetotails of Mars and Venus, *Adv. Space Res.*, *33*, 1945–1955.

Nagy, A. F., et al. (2004), The Plasma Environment of Mars, *Space Sci. Rev.*, *111*, 33–114, doi:10.1023/B:SPAC.0000032718.47512.92.

Vignes, D., C. Mazelle, H. Reme, M. H. Acuña, J. E. P. Connerney, R. P. Lin, D. L. Mitchell, P. Cloutier, D. H. Crider, and N. F. Ness (2000), The solar wind interaction with Mars: Locations and shapes of the bow shock and the magnetic pile-up boundary from the observations of the MAG/ER experiment onboard Mars Global Surveyor, *Geophys. Res. Lett.*, *27*, 49–52.

D. Brain, SSL/7 Gauss Way Space Sciences Lab, University of California, Berkeley, Berkeley, CA 94720, USA. (brain@ssl.berkeley.edu)

J. Cain and B. Ferguson, Geophysical Fluid Dynamics Institute, Florida State University, Tallahassee, FL 32306–4360, USA. (cain@gfdi.fsu.edu; bruce@geomag.gfdi.fsu.edu)

D. H. Crider, Physics Department, Catholic University of America, Washington, DC 20064, USA. (dcrider@lepvax.gsfc.nasa.gov)

E. Harnett, Department of Earth and Space Sciences, University of Washington, Box 351310, Seattle, WA 98195–1310, USA. (eharnett@u.washington.edu)